Astron. Astrophys. 317, 968–975 (1997)

ASTRONOMY
AND
ASTROPHYSICS

Radiative forces on lithium: effects of electron recoil and background opacities

J. Richer[1,2], **G. Michaud**[1,2], **and G. Massacrier**[3]

[1] CEntre de Recherche en Calcul Appliqué (CERCA), 5160 boul. Décarie, bureau 400, Montréal, Québec, H3X 2H9, Canada
[2] Département de Physique, Université de Montréal, Case Postale 6128, Succursale A, Montréal, Québec, H3C 3J7, Canada
[3] Centre de Recherche Astronomique de Lyon (UMR 142 du CNRS), École Normale Supérieure de Lyon, 46 allée d'Italie, F-69364 Lyon Cédex 07, France

Received 16 April 1996 / Accepted 11 June 1996

Abstract. Recent results on momentum transfer during photoionization processes determine how the ionizing photon momentum is split between the ejected electron and the recoiling ion. This leads to improved radiative force calculations. The consequences of this recoil for radiative forces are demonstrated by comparing for lithium the new accurate results with calculations based on simpler approximations commonly used in the past. We show that at some densities and temperatures typical of deep stellar envelopes, the total radiative force on lithium becomes negative (outgoing stellar radiation pushing the ions inwards); however this negative force is then negligible compared to gravity. In stellar envelope calculations, the exact results for hydrogenoid states are well approximated by the simpler formula that Sommerfeld obtained for the hydrogen 1s state. We also show that the force on Li depends significantly on the abundance of other elements, especially helium and oxygen, that block photon flux at critical wavelengths.

Key words: atomic processes – diffusion – radiative transfer – stars: abundances – stars: chemically peculiar

1. Introduction

In a recent article, Gonzalez et al. (1995b) presented a detailed description of the physics that must be taken into account in radiative force calculations for stellar envelopes. In the case of the force resulting from bound-free absorption, one important piece of information that was still missing is $f_{\rm ion}$, the fraction of the incident photon momentum that is actually transferred to the absorbing ion (the rest being carried away by the ejected electron). These authors used for any bound-free absorptions the simple formula (their Eq. (28)),

$$f_{\rm ion}({\rm H1s}) = 1 - \frac{8}{5}\left(1 - \frac{\nu_{\rm thres}}{\nu}\right) , \qquad (1)$$

where ν is the photon frequency, and $\nu_{\rm thres}$ the frequency at threshold. This formula had been obtained by Sommerfeld & Schur (1930) for the particular case of *the ground state of hydrogen*.

Until now most researchers relied implicitly or explicitly on the pure dipolar photoionization differential cross section for which $f_{\rm ion} = 1$. But particle momenta after photoionization can be much larger than the incident photon momentum, by a factor $2c/v$ in the non-relativistic regime (with c and v the light and photoelectron speeds respectively), thus greatly amplifying the effects of any small anisotropies that might be present in the photoelectron angular distribution. This point was stressed by Michaud (1970) who suggested that this simple formula (Eq. (1), which we will simply call the H1s formula) would be better than using $f_{\rm ion} = 1$ even for non-hydrogenoid photoionizing ions. It shows that $f_{\rm ion}$ can become negative (then the ions are pushed back, not forward, by radiation), and that deviations from unity become important already for energies not very far from threshold.

As a result of this, the possibility arises that some chemical elements might experience *negative* net radiative forces at certain depths in stars. This requires that bound-free absorptions dominate bound-bound ones. This has been suggested by Unglaub & Bues (1996) to be the case in hot high gravity stars; they however used $f_{\rm ion} = 1$ in most cases. Gonzalez et al. (1995b) had already demonstrated that $f_{\rm ion}$ (in the simple H1s approximation) can lead to an *important reduction* of the net radiative force on an abundant element (cf. their Fig. 7).

Massacrier (1995) presented recently new analytic expressions that allow hydrogenic photoionization cross sections and $f_{\rm ion}$s to be calculated *easily* for any state. This prompted us to examine the rôle played by $f_{\rm ion}$ in stellar envelope conditions. Here we apply his exact formulæ to the element lithium (Sect. 2),

Send offprint requests to: G. Michaud,
E-mail: michaudg@cerca.umontreal.ca

whose radiative acceleration at high temperature has been suggested to explain the Li gap observed in clusters (Michaud 1987; Richer & Michaud 1993, hereafter referred to as RM). Even if most of the Li radiative lift normally comes from bound–bound absorption, it is important to determine how bound-bound and bound-free absorption compare as the temperature is increased, and at what temperature the inversion of the total force begins to take place. Using new *numerical* results from Massacrier & El-Murr (1996), the effect of $f_{\rm ion}$ in neutral Li and Li^{+1} is also evaluated. In Sect. 2.3, we show that the H1s formula is sufficiently accurate for trace elements in their hydrogenoid state of ionization; we also show that in a slightly modified form, it reproduces very well the exact results of Massacrier for hydrogenoid excited states.

In Sect. 3, we illustrate the subtle coupling that may exist between the radiative force on one element (here, lithium), and the abundances of other elements. The particular case treated here demonstrates that for accurate predictions of element stratification in stellar envelopes, and for predicting surface abundances, it may often be necessary to compute detailed spectra of all the elements present in significant amounts as well as the time evolution of the abundances, in order to take into account the competition for photons between the various chemical elements.

2. Radiative force from photoionization

The starting point is the general expression for the momentum transfer rate due to photoionization between a radiation field of specific intensity $I_\epsilon(\boldsymbol{p}_\gamma)$ (photon polarization vector $\boldsymbol{\epsilon} \in \{\boldsymbol{\epsilon}_1, \boldsymbol{\epsilon}_2\}$, photon momentum $\boldsymbol{p}_\gamma = \frac{h\nu}{c}\boldsymbol{n}_\gamma$), and atoms or ions of species A, in initial ionization state $+(i-1)$ and internal quantum state j, recoiling after ionization in some direction $\boldsymbol{n}_A$ with momentum $\boldsymbol{p}_A$. The corresponding differential cross section is noted: $\frac{d\sigma_{i-1,j}}{d\Omega_A}(\boldsymbol{p}_\gamma, \boldsymbol{\epsilon}\,; \boldsymbol{n}_A)$. After summing over states j, frequencies ν, polarizations $\boldsymbol{\epsilon}$, and directions $\boldsymbol{n}_\gamma$ and $\boldsymbol{n}_A$ (photon and ion directions within solid angles $d\Omega_\gamma$ and $d\Omega_A$ respectively), one obtains the mean momentum transfer per unit time and unit volume, which is assumed to be shared uniformly among all A^{+i} ions. This is equivalent to a *radiative force* acting directly on every A^{+i} ion in the unit volume. For the purpose of comparing this force to gravity, which is usually the main force present, it is useful to write it as the ionic mass m_A times a radiative *acceleration*, $\boldsymbol{g}^{\rm rad}_{\text{b-f},i}$, which is then given by:

$$N_i\, m_A\, \boldsymbol{g}^{\rm rad}_{\text{b-f},i} = \sum_{j,\epsilon} N_{i-1,j} \times \int d\nu \oint d\Omega_\gamma \frac{I_\epsilon(\boldsymbol{p}_\gamma)}{cp_\gamma} \oint d\Omega_A \frac{d\sigma_{i-1,j}}{d\Omega_A}(\boldsymbol{p}_\gamma, \boldsymbol{\epsilon}\,; \boldsymbol{n}_A)\, \boldsymbol{p}_A, \quad (2)$$

where $N_{i-1,j}$ is the number density of absorbers of charge $+(i-1)$ in state j, and N_i the number density of ions of charge $+i$ in any excitation state.

In the summation on j in the latter equation, one can group together (defining a level) those internal quantum states j that are degenerate due to the spherical symmetry of the ion Hamiltonian. For absorbers that are randomly oriented, those states are equally populated. Using the fact that the differential cross section does not change when $-\boldsymbol{\epsilon}$ replaces $\boldsymbol{\epsilon}$, one can show that when averaged on such a level the integral on $d\Omega_A$ results in a vector that is parallel to the photon incident momentum $\boldsymbol{p}_\gamma$. Considering now j as a label for the levels, the (averaged) integral might be replaced by $\sigma_{i-1,j}(\nu) f_{\rm ion}^{i-1,j}(\nu)\boldsymbol{p}_\gamma$, where $\sigma_{i-1,j}(\nu)$ is the total cross section, thus defining $f_{\rm ion}$. One obtains:

$$\begin{aligned} N_i\, m_A\, \boldsymbol{g}^{\rm rad}_{\text{b-f},i} &= \sum_{j,\epsilon} N_{i-1,j} \int d\nu \oint d\Omega_\gamma \frac{I_\epsilon(\boldsymbol{p}_\gamma)\boldsymbol{n}_\gamma}{c} \sigma_{i-1,j}(\nu) f_{\rm ion}^{i-1,j}(\nu) \\ &= \sum_j N_{i-1,j} \int_0^\infty \frac{\mathscr{F}_\nu}{c} \sigma_{i-1,j}(\nu) f_{\rm ion}^{i-1,j}(\nu)\, d\nu. \end{aligned} \quad (3)$$

In stars, the energy flux $\mathscr{F}_\nu$ is normally radial; then so is the radiative acceleration and vector notation is usually dropped at this stage.

When the flux appearing in Eq. (3) is estimated using the diffusion approximation, in a star of effective temperature $T_{\rm eff}$ and radius $R_\star$, at a point where the Rosseland mean opacity is $\overline{\kappa}_R$, and the total monochromatic opacity is $\kappa(u)$, ($u \equiv h\nu/kT$), Eq. (3) can be rewritten as

$$g^{\rm rad}_{\text{b-f},i} = \frac{(kT_{\rm eff})^4}{(4\pi)^2(\hbar c)^3} \left(\frac{R_\star}{r}\right)^2 \frac{\overline{\kappa}_R}{N_i m_A} \times \sum_j \int_0^\infty \frac{N_{i-1,j}\sigma_{i-1,j}(u) f_{\rm ion}^{i-1,j}(u)}{\kappa(u)} P(u)\, du\,, \quad (4)$$

where $P(u) \equiv u^4 e^u/(e^u-1)^2$. For practical computations, it is useful to separate the lithium contribution to $\kappa(u)$ from the remaining background opacity $\kappa_c(u)$ and rewrite the second line in Eq. (4) as

$$\rho \int_0^\infty \frac{\sum_j \kappa_{i-1,j}(u) f_{\rm ion}^{i-1,j}(u)}{\kappa_c(u) + \kappa_{\rm Li}(u)} P(u)\, du, \quad (5)$$

where ρ is the local mass density, $\kappa_{i-1,j} = N_{i-1,j}\sigma_{i-1,j}/\rho$, and $\kappa_{\rm Li}(u)$ is the total lithium monochromatic opacity (including line and continuous opacities of all its ions).

2.1. Discussion of $f_{\rm ion}$

The differential cross section $\frac{d\sigma_{i-1,j}}{d\Omega_A}(\boldsymbol{p}_\gamma, \boldsymbol{\epsilon}\,; \boldsymbol{n}_A)$ for incident photon momentum $\boldsymbol{p}_\gamma$ and polarization $\boldsymbol{\epsilon}$ may be obtained from the photoelectron differential cross section $\frac{d\sigma_{i-1,j}}{d\Omega_e}(\boldsymbol{p}_\gamma, \boldsymbol{\epsilon}\,; \boldsymbol{n}_e)$ through kinematical relations; the calculation of this last cross section was recently improved upon by Massacrier (1995) and Seaton (1995). Seaton gives results only for hydrogenoid states up to 3d, whereas Massacrier gives expressions for any hydrogenoid state. Massacrier & El-Murr (1996) also give results for neutral Li and Li^{+1}. Our work has been based entirely on the results of Massacrier and El-Murr.

Up to electric dipole order in the photon–atom interaction Hamiltonian, the averaged electron recoiling angular distribution has axial symmetry around the polarization vector, and inversion symmetry with respect to the origin (Sommerfeld 1939);

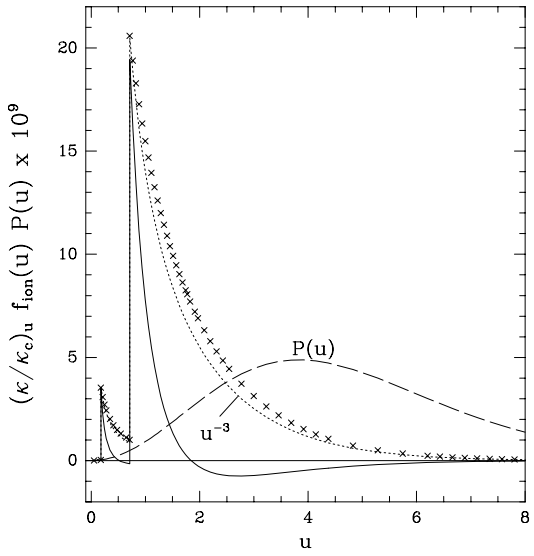

Fig. 1. Photon momentum transferred to Li^{+3} through Li^{+2} photoionization at a given frequency, per unit time and volume, in dimensionless units, for a *constant* background opacity κ_c. *Solid line*: calculation based on Massacrier's formulæ. *Crosses*: same with $f_{\rm ion} = 1$. *Dotted line*: calculation based on the classic u^{-3} law with $f_{\rm ion} = 1$. *Dashed line*: spectrum $P(u)$ of black body momentum flux; $u \equiv h\nu/kT$. Li concentration by number is 10^{-9}. The temperature is 2×10^6 K.

after averaging over angles no momentum is imparted to the electron, in the ion-electron center-of-mass frame, even for polarized light. This symmetry is broken if one includes the next order in the transition matrix elements. The resulting electric dipole–quadrupole interference terms in the differential cross section shift the electron distribution forward or backward, in the $\boldsymbol{p}_\gamma$ direction. The mean momentum $\langle \boldsymbol{p}_{\rm e}\rangle \equiv f_{\rm e}\boldsymbol{p}_\gamma$ taken up by electrons (necessarily parallel to $\boldsymbol{n}_\gamma$, by symmetry) has approximately the same value in both the center-of-mass and gas frames, provided all energies are $\ll m_e c^2$; the photon momentum fraction transferred to the *ion* is then given by $f_{\rm ion} = 1 - f_{\rm e}$, in the gas frame.

Massacrier (1995) has considered the case of one-electron ions and derived the differential cross section taking quadrupolar contributions into account. He gave convenient new expressions to evaluate $\sigma_{n\ell}(\nu)$ and $f_{\rm ion}^{n\ell}(\nu)$ in Eq. (3) for an hydrogenoid absorber in any level $n\ell$. More recently, Massacrier & El-Murr (1996) have extended the application of Massacrier's quantum analysis to neutral Li and Li^{+1}. Using Quantum Defect Theory, they were able to compute numerically $f_{\rm ion}$s for these ions, and we have used these results, together with photoionization cross sections from the TOPbase database (Cunto et al. 1993), to evaluate radiative forces due to bound-free absorptions on these ions.

To demonstrate the effect of a properly calculated $f_{\rm ion}$, Fig. 1 shows the value of the integrand in Eq. (5) for the photoionization of Li^{+2} (resulting in a force on Li^{+3}), for a constant background opacity $\kappa_c(u) = \overline{\kappa}_R = 10.5\,{\rm cm}^2/{\rm g}$, when the lithium concentration by number is 10^{-9}, at a point in a stellar envelope where $T = 2\times10^6$ K. At such a low concentration, the Li contribution to opacity, $\kappa_{\rm Li}(u)$, is negligible compared to $\kappa_c(u)$, and the resulting acceleration on lithium is independent of concentration. The envelope parameters are those of a main sequence star with $T_{\rm eff} = 8000$ K, $\log g_{\rm surface} = 4.4$, $Y = 0.292$ and $Z = 0.02$.

The absorption edge at $u \sim 0.7$ is that of the ground state of Li^{+2}. Excited states of Li^{+2} with $n > 2$ are strongly depopulated by pressure ionization and make no significant contribution. Integration of the exact result (*solid* line) over frequency leads to almost complete cancellation of the bound-free force, in contrast to what would result from the integration with $f_{\rm ion} = 1$ (*crosses*). Note also the difference between the *crosses* and the *dotted* line, which shows essentially the difference between exact hydrogenic cross sections and the classic ν^{-3} law.

2.2. Detailed computations

Except for these new values of $f_{\rm ion}$, details of the computation of the radiative acceleration of lithium in stellar envelopes, including bound-free and bound-bound contributions, are somewhat standard.

In this paper, ionization equilibrium and excited state populations are calculated following the prescription of Hummer & Mihalas (1988). The background opacity $\kappa_c(u)$ is calculated at each depth of the envelope model from tables of monochromatic opacities (based on TOPbase data) for H, He, C, N, O, Fe (Gonzalez et al. 1995a, 1995b) and Si (LeBlanc 1996) providing an energy resolution of $0.005\,kT$. In order to compensate for the missing elements [the envelope models had metals in solar proportions, and were based on OPAL and Kurucz's opacities (Rogers & Iglesias 1992; Kurucz 1990)], we chose to scale the total $\kappa(u)$ uniformly so that its Rosseland mean agrees with that used in the models at the same depth. The typical correction to $\kappa(u)$ is about ±15 % below $T = 10^5$ K, but rises to as much as a factor of 2.5 deeper in the star. This is the main source of uncertainty in our calculations, and it can only be reduced by adding more elements, increasing the frequency resolution of our grid and treating Fe term splitting more accurately than is done in TOPbase. With this rough correction factor, the radiative forces at $T \gtrsim 10^6$ K should be accurate to about a factor of two. Results are much better at lower temperature where radiative accelerations matter most, because of the much shorter diffusion time scales ($< 10^9$ yr).

The bound-free and bound-bound contributions to the radiative acceleration of lithium are computed with data taken from the TOPbase database, except for $f_{\rm ion}$ which was discussed above. For the bound-bound contribution, line broadening is accounted for by semiempirical formulæ as in Gonzalez et al. (1995b); the momentum absorbed is redistributed among the ions in a way analogous to that described by Michaud et al. (1979) for helium. For the bound-free part, excited states with (optical electron) principal quantum number $n \leq 6$ are included.

Two comments must be made here concerning TOPbase data. First, TOPbase photoionization cross sections cover only about one decade in energy above threshold. This turns out to

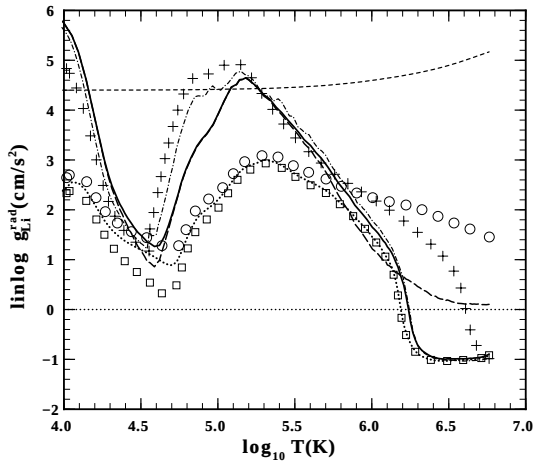

Fig. 2. Radiative acceleration of lithium in the envelope of a 8 000 K main sequence star. *Long dash*: line absorption; *dotted*: continuous absorption; *solid*: total; *dot-dash*: total, but for an helium poor envelope (see § 3); these are "exact" results. Some approximations: *crosses*: total, using $\kappa_c(u) = \kappa_{\rm Bors}(u)$; *squares*: continuous absorption calculated with $f_{\rm ion}$(H1s) for all bound-free absorptions; *circles*: continuous absorption calculated with $f_{\rm ion} \equiv 1$. *Short dash*: local gravity (for the homogeneous envelope). The function "linlog" is defined in the text.

be insufficient to investigate the sign inversion in bound-free forces; in some cases the bound-free contribution is strongest and negative far above threshold, and is missed if TOPbase data are not extended to higher energies. So we extended the cross section data to about 100 $\nu_{\rm thres}$ by adding a few values along each final log-log asymptote. Second, TOPbase photoionization cross sections start a little below threshold; these extra values replace, in the database, all those absorption lines that would normally be merging near the ionization limit; we assigned $f_{\rm ion} \equiv 1$ to all such points below threshold, assuming they represent in fact bound-bound transitions.

The results of the full $g_{\rm Li}^{\rm rad}$ calculation are presented[1] in Fig. 2. It shows the outcome of various approximations for $\kappa(u)$ and $f_{\rm ion}$, some of which will be discussed in Sect. 3.

Two different envelope models were used in Fig. 2. One is homogeneous, with $Y = 0.292$ (we will refer to it as the *normal* He model). The other was chosen to illustrate the effect of helium sinking on $g_{\rm Li}^{\rm rad}$; it has $Y \approx 10^{-4}$ from the surface down to $T \sim 1.1 \times 10^6$ K, where Y rises smoothly to $Y = 0.292$. The two envelopes were computed with the envelope code described by Richer et al. (1992), with OPAL opacities. The envelopes correspond to ZAMS stars with slightly different masses (~ 1.70 and $\sim 1.76\,{\rm M}_\odot$, respectively), chosen so that their effective temperatures be about 8 000 K in both cases (surface He gravitational settling lowers $T_{\rm eff}$).

[1] The function "linlog" used in some of the figures is defined by

$$y = \text{linlog}(x) \quad \Longleftrightarrow \quad x = 10^y - 10^{-y};$$

it is a kind of base 10 arcsinh function, useful for displaying both large and small, positive and negative values of the same function. For $|x| \gtrsim 8$, $\text{linlog}(x) \approx \text{sign}(x) \cdot \log_{10}|x|$, and for $|x| < 1$, $\text{linlog}(x) \sim x/5$.

The main factor that determines how an element is stratified throughout a convectively stable non rotating envelope, is the difference between its total radiative acceleration and local gravity, g; for that reason the latter is shown in Fig. 2, as the *short dash* line near the top of the figure. This curve is from the $Y = 0.292$ model. In the inhomogeneous He model, g is smaller by a factor 1.44 in layers with $T < 10^6$ K. The temperature range covered ends, on the right, at the envelope-core boundary.

The total radiative acceleration $g_{\rm Li}^{\rm rad}$ in the *inhomogeneous* He poor background is shown as the *dot-dash* curve; it will be discussed in Sect. 3. All other $g_{\rm Li}^{\rm rad}$ results pertain to the normal He model. Curves represent exact calculations; symbols represent approximations. The *solid* line gives the total radiative acceleration, based on the detailed frequency dependent $\kappa(u)$. It includes bound-bound transitions (shown separately as the *long dash* line) and bound-free absorptions (*dotted* line). Curves with a bound-bound contribution show small scale irregularities; they appear whenever new strong Li lines enter the frequency integration domain at the upper boundary $u = 20$; the minimum upper limit necessary to render such jumps unnoticable seems to be $u = 25$, but the $u = 20$ limit was imposed to us by the Gonzalez et al. (1995a) tables.

Circles give the Li bound-free contributions when $f_{\rm ion}$ is set equal to one. This overestimates $g_{\rm b\text{-}f}^{\rm rad}$ by at least 25 % everywhere, and is completely wrong at high temperatures, as could be predicted from Fig. 1.

Squares represent the Li bound-free contribution when $f_{\rm ion}$(H1s) is used for all Li states. This is a good approximation for high temperatures (compare with the *dotted* line); however one can see that it underestimates the continuum contribution for $\log T \lesssim 5.1$, with largest error near $\log T = 4.6$. If calculated exactly, the bound-free contribution compares at this temperature to the bound-bound one (*long dash*), while when using $f_{\rm ion}$(H1s), it is strongly reduced. Li is present there mostly as the He-like ion Li^{+1} but receives all of its very weak lift while in the neutral state (the method used for averaging contributions from different ionization states is described by Gonzalez et al. (1995b)). The ns states of neutral Li have $f_{\rm ion}$s that are quite different from those of all other Li states (Massacrier & El-Murr 1996); just above threshold they reach values significantly greater than 1 before dropping slowly below zero, while in other states $f_{\rm ion}$ either drops immediately towards negative values (like $f_{\rm ion}$(H1s)), or rises only very slightly above 1 before dropping. For lithium this appears to be the largest deviation from the $f_{\rm ion}$(H1s) type of behaviour. It is unimportant in our envelope models: neutral Li is never the dominant state of ionization, and when the deviation affects the radiative acceleration, the latter is only a small fraction of the local gravity.

Such a deviation of $f_{\rm ion}$s from the $f_{\rm ion}$(H1s) type could have more important implications if it occurs for dominant ionization states of abundant elements like C, N or O (see Sect. 3). Quantum Defect Theory suggests that the deviation is negligible for atomic states with small quantum defects. The latter globally decrease with increasing ionic charge. Thus for these deviations to have any quantitative importance on radiative accelerations,

the element would have to be predominantly in a close shell state (so that bound-bound absorption does not dominate), with its less ionized neighbouring absorbing state close to *neutral* for the deviation to be significant. The largest deviations from a hydrogenoid behaviour regarding $f_{\rm ion}$s should consequently be found only in cool surface layers, where ionization states of elements are not too high. Hence as an approximation for stellar *interiors*, the $f_{\rm ion}$(H1s) formula might be more widely applicable than previously thought. We emphasize that such a conclusion can be only temporary and deserves computations of $f_{\rm ion}$s for atomic states beyond the reach of the simple Quantum Defect Theory as used in Massacrier & El-Murr (1996).

The last approximation shown in the figure (*crosses*) is a calculation of the total radiative acceleration in which all Li contributions are treated exactly, but where the complicated background opacity $\kappa(u)$ is replaced by the simple fit $\kappa_{\rm Bors}(u)$ of Borsenberger et al. (1979). This fit mimics the absorption edge of ground state hydrogen, and assumes $\kappa_c(u) = \overline{\kappa}_R$ at higher energies. Coupled evolution–diffusion calculations by RM used this approximation together with $f_{\rm ion} = 1$. Here, $f_{\rm ion}$ is exact. The result is quantitatively rather bad (compare *crosses* and the *solid* line), but it turns out that it is very good in the small temperature range near $\log T = 5.3$ that is most important to the Li gap problem (the formation of the Li gap in cluster stars is explained by Michaud (1986) and RM in terms of diffusion). For $\log T < 5.1$ the agreement becomes better when one compares with the model where no He is present (*dot-dash* line); this is further discussed in Sect. 3.

2.3. Simple formula for the hydrogenic case

For any shell n of an *hydrogenoid* ion of nuclear charge Z, the simple formula (with ε defined below)

$$\frac{1}{n^2}\sum_{\ell=0}^{n-1}(2\ell+1)\sigma_{n\ell}f_{\rm ion}^{n\ell} \approx 0.226\, n^{1+\varepsilon}\frac{a_0^2}{Z^2}\left(\frac{\nu_n}{\nu}\right)^3\left[1-\frac{8}{5}\left(1-\frac{\nu_n}{\nu}\right)\right], \qquad (6)$$

where a_0 is the Bohr radius and $h\nu_n$ the ionization energy of the shell, was found to be a good approximation for the sum over subshells ℓ that is implicit in the numerator of Eq. (5). The expression on the right hand side is (without the ε) the classical expression for the cross section, multiplied by the exact value of $f_{\rm ion}$ for the 1s state (Eq. (1)); the numerical factor includes a factor of 0.8 for the Gaunt factor of the 1s state at threshold (Allen 1973).

This is compared in Fig. 3 (*solid* line) to some exact results (*dot(s)-dash*) for $n = 1$ to 4, and to the classic expression for the $n = 1$ state. Exact results with $n > 4$ are almost indistinguishable from the $n = 4$ curve. The exact calculations have been normalized to a common value at threshold, by multiplication by a factor $n^{-\varepsilon}$, with $\varepsilon \approx 0.08$. This factor (obtained by eye fitting) was introduced to improve the fit to a common curve; it absorbs most of the differences at threshold, between curves of different n, that would normally be attributed to the n

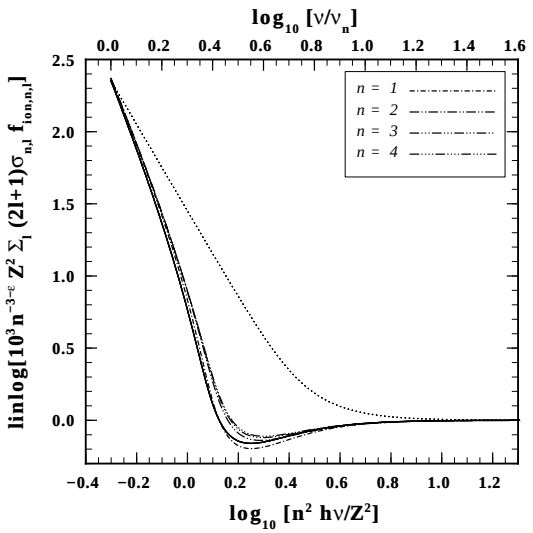

Fig. 3. Normalized hydrogenoid momentum transfer cross sections for photoionization from different excited levels of threshold frequencies ν_n (*dot(s)–dash*), and approximate formula (*solid line*) of Eq. (6). The classic expression in ν^{-3}(with $f_{\rm ion} = 1$) is also shown (*dotted*). The exponent ε is defined in the text. Atomic units are used throughout.

dependence of a Gaunt factor. Note the important change in the slope near threshold, due mostly to $f_{\rm ion}$: the energy dependence is changed from ν^{-3} to $\nu^{-4.6}$.

For lithium, using expression (6) is almost equivalent to using $f_{\rm ion}$(H1s) with exact cross sections, and very similar results are obtained with Eq. (6) with fewer calculations (the sum over angular momentum substates is already included in this formula). Part of the success of these approximations (compare the *dotted* line and *squares* in Fig. 2; neutral Li and Li^{+1} can be ignored above $\log T \gtrsim 5.2$) comes from the fact that bound-free absorption in Li^{+2} takes place mostly in the ground state, even at high temperatures. For example, assuming no saturation, $f_{\rm ion} = 1$, using the classical photoionization formula, a frequency independent background opacity and Boltzmann ratios for the populations, one finds for the ratio of the $n = 2$ hydrogenoid contribution to the ground state one:

$$\frac{g_{\rm b\text{-}f}^{\rm rad}(n=2)}{g_{\rm b\text{-}f}^{\rm rad}(n=1)} = 2^3\,\frac{S(u_2)}{S(u_1)}, \qquad (7)$$

where

$$u_n = \left(\frac{Z}{n}\right)^2\frac{1.578\times10^5}{T(\rm K)},$$

and

$$S(u) = u^3\left\{\frac{u}{1-e^{-u}} - e^u\ln(1-e^{-u})\right\};$$

for lithium, this ratio never exceeds 17 % at any temperature[2].

[2] Note that using the Hummer & Mihalas (1988) formalism would further reduce the contribution of excited states.

Massacrier's (1995) exact formulæ are not too difficult to program, but they can use up a lot of computing time, if the calculations need to be done repeatedly; so Eq. (6) should be useful if accurate tables are not available. Massacrier also proposed simple rational approximations in photon energy (his Eqs. (52) to (55)) that are a good fit to his exact $f_{\rm ion}$s for every hydrogenic subshells $n\ell$; use of these formulæ together with the classic ν^{-3} law for cross sections provides an alternative to Eq. (6), but each subshell ℓ of a shell n would have to be computed separately.

A different approach for computing radiative forces due to photoionization was proposed by Alecian (1994). It is based on two-parameter quasi-hydrogenic cross sections. Important savings in computation time are made possible by his factorization of the radiative acceleration of each ion into a simple model dependent factor and a model independent function of temperature, all the ion atomic physics being lumped into the latter. Alecian used $f_{\rm ion}$ = 1 and $f_{\rm ion}$ = $f_{\rm ion}$(H1s) only, but Massacrier's formulæ and numerical data could very well be used instead to define and tabulate these functions of T. This approach is applicable to trace elements only, and cannot, at least in its present form, yield better results than our calculation with $\kappa(u) = \kappa_{\rm Bors}(u)$, as it assumes $\kappa_c(u) = \overline{\kappa}_R$ for all temperatures and frequencies. For abundant elements or for more accurate work, integration over frequencies cannot be avoided, as will be shown in Sect. 3, but one could still make use of quasi-hydrogenic cross sections and use exact $f_{\rm ion}$s or Eq. (6) to adjust Alecian's parameters and reproduce the correct slopes near threshold. One would then expect reductions in the bound-free force similar to those visible in Fig. 2.

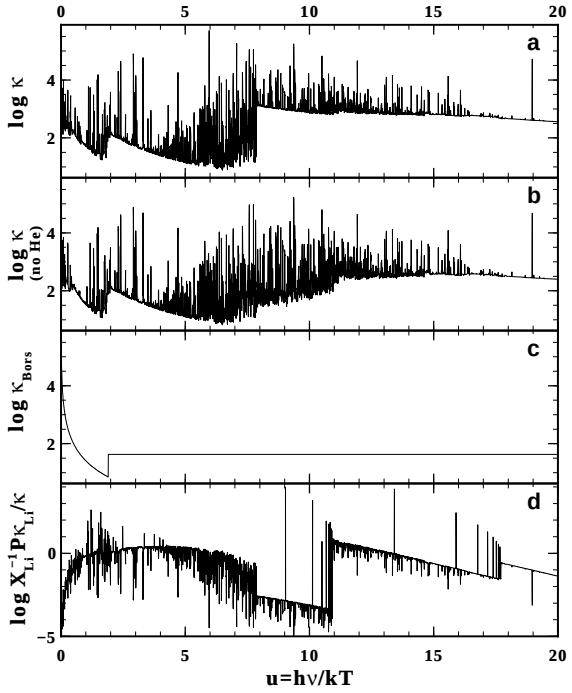

Fig. 4a–d. Monochromatic opacities at $\log T$ = 4.9. **a** Total opacity, including the contributions of H, He, C, N, O, Si, Fe and Li for the homogeneous model (Y = 0.292). **b** Same as **a** but with Y reduced to 10^{-4}. **c** The Borsenberger et al. (1979) approximation to $\kappa(u)$. **d** Normalized energy flux absorbed by Li, with the background opacity of **a**. In **d**, the stronger lines below u = 13 belong to Li^{+1}; lines at $u > 13$ belong to Li^{+2}.

2.4. Effect of uncertainties in occupation levels

At many temperatures, the bound-free contributions of most states with $\ell > 0$ is negative while the contribution of the ground state is positive. The question arises as to how dependent the relative values of the positive and negative contributions is on the occupation of the levels and on our use of the Hummer & Mihalas (1988) formalism. Consider for instance $\log T$ = 6.0, where all excited states of Li^{+2} with $\ell > 0$ contribute negatively to the force, while the ground state contribution is positive. Some *crude* calculations were made using the occupation probabilities w_n of Iglesias & Rogers (1995; their Table 1)[3] instead of those of Hummer & Mihalas; there resulted higher excited state populations, and an 8 % reduction in the bound-free force, but the reduction mostly reflected the drop in the ground state population. Similarly, by forcing w_n = 1 for all states (of all ions; this assumption was made also in Eq. (7)), excited states of Li^{+2} became even more populated, at the expense of the ground state, but their contributions remained negligible; the ground state contribution, and the total bound-free force, dropped by a factor of $\sim$ 3. So unless extreme and unrealistic conditions (for a stellar plasma) are imposed, the ground state contribution is always the only one that matters for *hydrogenoid* Li. Bound-bound absorption is usually much more important than bound-free absorption for neutral Li and Li^{+1} so for them the question of cancellation between positive and negative bound-free absorptions is less important.

3. Coupling between lithium and other elements

Fig. 4 shows monochromatic opacities at $\log T$ = 4.9 and allows to understand how other chemical species influence $g_{\rm Li}^{\rm rad}$. This is in the temperature range where $g_{\rm Li}^{\rm rad}$ is most sensitive to the He abundance (see Fig. 2). Fig. 4a shows the total monochromatic opacity when Y=0.292 ($\overline{\kappa}_R$=37.0 cm^2/g); Fig. 4b shows the same quantity when helium has sunk towards hotter regions (Y=10^{-4}, $\overline{\kappa}_R$=30.6 cm^2/g). In both cases, $\kappa(u)$ was scaled to obtain the Rosseland mean opacity used in the models but that

The same calculation can also be done with $f_{\rm ion}$=$f_{\rm ion}$(H1s); $S(u)$ now becomes

$$S(u) = u^3 \left\{ \frac{u}{1-e^{-u}} + \frac{3}{5} e^u \ln(1-e^{-u}) \right\} .$$

This function becomes negative for $u \lesssim 0.27$ and the ratio in Eq. (7) becomes very large when $u_1 \approx 0.27$. However it is still true that $g_{\rm b\text{-}f}^{\rm rad}(n=1)$ is a sufficient approximation to the total bound-free force on Li^{+2}; the contributions of states with $n > 1$ remain small in absolute value, and only shift slightly the temperature at which $g_{\rm b\text{-}f}^{\rm rad}$=0.

[3] These were intended for another element and slightly different plasma conditions, but according to these authors, the pattern of departure between them and those of Hummer & Mihalas (1988) should be typical.

Table 1. Some spectral line coincidences between Li and O

state(λ, Å)	state(λ, Å)	gf
Li II(172.5)	O V(172.5)	0.394
Li II(168.1)	O V(168.2)	0.485
Li II(167.2)	O V(167.3)	0.096
	O V(167.4)	0.285
Li II(166.6)	O IV(166.6)	0.013

correction was less than 1 % in each case. These quantities appear in Eq. (5) and determine what fraction of the flux is available to support Li. The normalized energy flux absorbed by Li is shown at the bottom of Fig. 4d; it includes the Planck flux factor $P(u)$, and is normalized to $X(\mathrm{Li}) = 1$; the background opacity used is that of Fig. 4a. The lines near the center ($u \sim 10$), and most of the lines on the left belong to Li^{+1}, while the ones at $u > 13$ form Li^{+2}'s Lyman series; at this temperature, most Li atoms ($\sim 90\,\%$) are in the Li^{+2} ground state.

Lithium has no strong lines near the maximum of the function $P(u)$ (at $u \sim 4$), where the background opacity would be close to the Rosseland mean opacity; so its acceleration is mainly affected by details of the background spectrum that have little effect on the envelope model. In this case, most of the force comes from the lines near $u \sim 10$, which fall in the region of He II continuum absorption. Most of the flux that is blocked by He in the He-normal envelope becomes available to these Li lines when He disappears, and $g_{\mathrm{Li}}^{\mathrm{rad}}$ is then increased by about one order of magnitude! It changes from $g_{\mathrm{Li}}^{\mathrm{rad}} < g$ to $g_{\mathrm{Li}}^{\mathrm{rad}} > g$ over a significant interval of T, which will translate into important abundance changes at the surface of the star. In stellar envelopes, diffusion time scales for Li and He are comparable, so changes in Li abundances will have to be considered simultaneously with changing He abundance profiles if predictions are to be reliable.

Fig. 4c allows us to understand why the approximation $\kappa(u) \approx \kappa_{\mathrm{Bors}}(u)$ gave better results in the helium poor envelope than in the normal helium envelope (see Fig. 2 and the end of Sect. 2.2). By definition, $\overline{\kappa}_R$ is always a reasonable approximation to the background opacity near the maximum of $P(u)$, whatever the envelope composition. In the Borsenberger et al. approximation, this value of the opacity is extended all the way to infinite energies, while a look at Fig. 4a shows clearly that $\kappa(u \sim 4)$ differs greatly from $\kappa(u \sim 10)$ for the homogeneous envelope. They differ in fact by nearly two orders of magnitude. When there is no helium (Fig. 4b), the disagreement is not so pronounced.

A closer examination of the individual element contributions to $\kappa(u)$ reveals that many of the strong Li lines coincide with strong oxygen lines, at the resolution of our calculations (see Table 1). There are also a few coincidences with iron lines. Vauclair (1988) lists several other coincidences, some of which involve elements not considered here (Ne, Mg). These overlapping lines will add some coupling between the radiative force on Li and the abundance of these elements.

4. Conclusion

From the results of Sect. 2, one can conclude that for lithium, 1) the f_{ion} factor cannot be ignored when one is interested in the bound-free force; 2) the bound-free contribution is very small compared to the line contribution, except when Li is in the Li^{+1} He-like configuration, around $\log T = 4.5$, or at the highest temperatures, where the element is almost completely ionized (note that Li is rapidly consumed by nuclear reactions with protons if $\log T > 6.4$); 3) at these highest temperatures, the backward force from photoionization is greater than the forward force transmitted through the lines, and radiation *pulls* the element towards the stellar center; 4) the bound-free force is always small compared to gravity, and it could be ignored altogether; its largest contributions are reasonably well approximated when Eq. (1) is used for all bound-free absorptions (or Eq. (6), for hydrogenoid states).

Perhaps more important for radiative force calculations is the realization that a strong coupling can exist between the force on one element and the abundance of another one. This coupling occurs when the lines or continous absorption of an abundant element block the radiation flux in strong lines of the other. It was shown in Sect. 3 that at some temperatures the radiative force on lithium increases by a large factor, through this mechanism, when helium settles gravitationally towards hotter regions. The increased force will lead to significant changes in the evolution of the lithium distribution in and at the surface of radiative stellar envelopes.

Saturation of absorption lines is a manifestation of the same phenomenon (with the same abundant element in both rôles). When an ion is sufficiently abundant in a region of the star for its strong lines to become saturated, the contribution of its continuous absorption, which is much less subject to saturation, increases in relative importance. For abundant elements like C, N, O and Fe, it can become a sizable fraction of the total radiative force, as was demonstrated by Gonzalez et al. (1995a, 1995b). When continuous absorption from the ground state begins to saturate also, excited levels could begin to contribute more strongly. For these levels the f_{ion}(H1s) formula used by these authors in their best calculations, may no longer provide a sufficiently good approximation. Some f_{ion}s might show large deviations of the type encountered in neutral Li(ns) states (see Sect. 2.2). This will be especially important at high temperatures where these elements are the main source of opacity.

One can simulate such a situation in the case of lithium by raising concentration levels to X(Li) $\sim$ 0.1–0.5, to make it one of the major absorbers. Then the force from line absorption drops to a level that is everywhere comparable in strength to continuous absorption, while ground state Li^{+2} bound-free absorption begins to saturate for $\log T \gtrsim 5.3$. The negative contributions from its excited states can now largely exceed, in relative magnitude, the 17 % limit that was estimated in Eq. (7) for $f_{\mathrm{ion}} = 1$. This causes the temperature at which $g_{\mathrm{b\text{-}f}}^{\mathrm{rad}}$(Li) becomes negative to drop to 1.3×10^6 K ($\log T = 6.1$).

This example suggests that a more accurate calculation of continuous absorption by C, N, O and Fe is necessary to verify

the reliability of currently used approximations, especially when they are extended to non-hydrogenoid ions.

Compared to the results of RM, where the Borsenberger et al. (1979) approximation was used for background opacities (shown as *crosses* in Fig. 2 of the present paper) the overall changes *reduce* the radiative acceleration on lithium at temperatures near 10^5 K. One then expects smaller overabundances of Li on the hot side of the Li gap than were predicted in RM (e.g., in Fig. (9) of that paper). The disappearance of He leads to quasi equality between gravity and $g_{\rm Li}^{\rm rad}$ over a significant temperature range, which should also tend to reduce variations of surface Li abundances with $T_{\rm eff}$ in F stars.

Acknowledgements. This research was supported by NSERC funds, and by a travel grant (G. Massacrier) from the Centre Jacques Cartier.

References

Alecian G., 1994, A&A 289, 885
Allen C. W., 1973, Astrophysical Quantities, 3rd edition, (London: Athlone Press)
Borsenberger J., Michaud G., Praderie F., 1979, A&A 76, 287
Cunto W., Mendoza C., Ochsenbein F., Zeippen C. J., 1993, A&A 275, L5
Gonzalez J.-F., Artru M.-C., Michaud G., 1995a, A&A 302, 788
Gonzalez J.-F., LeBlanc F., Artru M.-C., Michaud G., 1995b, A&A 297, 223
Hummer D. G., Mihalas D., 1988, ApJ 331, 794
Iglesias C. A., Rogers F. J., 1995, ApJ 443, 460
Kurucz R. L., 1990, private communication
LeBlanc F., 1996, private communication
Massacrier G., 1995, A&A, in press
Massacrier G., El-Murr K., 1996, submitted to A&A Letters
Michaud G., 1970, ApJ 160, 641
Michaud G., 1986, ApJ 302, 650
Michaud G., 1987, Phys. Scr. 36, 112
Michaud G., Montmerle T., Cox A. N., Magee N. H., Hodson S. W., Martel A., 1979, ApJ 234, 206
Richer J., Michaud G., 1993, ApJ 416, 312 (RM)
Richer J., Michaud G., Proffitt C. R., 1992, ApJS 82, 329
Rogers F. J., Iglesias C. A., 1992, ApJ 401, 361
Seaton M. J., 1995, J. Phys. B 28, 3185
Sommerfeld A. J. W., 1939, Atombau und Spektrallinien, Vol. 2, 5th edition, (Braunschweig: F. Vieweg)
Sommerfeld A. J. W., Schur G., 1930, Ann. Phys. (Leipzig) 4, 409
Unglaub K., Bues I., 1996, A&A 306, 843
Vauclair S., 1988, in *The Impact of Very High S/N Spectroscopy on Stellar Physics*, eds. G. Cayrel de Strobel, & M. Spite, IAU symposium 132, (San Francisco: PASPC), pp 463–467

This article was processed by the author using Springer-Verlag LaTeX A&A style file *L-AA* version 3.